Hybrid density-functional calculation of the electronic and magnetic structures of tetragonal CuO

Xing-Qiu Chen,[1] C. L. Fu,[1] C. Franchini,[2] and R. Podloucky[3]
[1]*Materials Science and Technology Division, Oak Ridge National Laboratory, Oak Ridge, Tennessee 37831, USA*
[2]*Faculty of Physics, Universität Wien and Center for Computational Materials Science, A-1090 Wien, Austria*
[3]*Institute for Physical Chemistry, University of Vienna, Sensengasse 8/7, A-1090 Wien, Austria*
(Received 21 April 2009; revised manuscript received 2 July 2009; published 28 September 2009)

The electronic and magnetic properties of recently synthesized tetragonal CuO with $c/a>1$ is calculated by means of hybrid density-functional theory. We predict that this tetragonal phase orders antiferromagnetically and has an exceptionally high Neél temperature $T_N \approx 800$ K, which makes it an ideal candidate for doping experiments and a potential parent of superconductors. The electronic structure is characterized by a charge-transfer gap of 2.7 eV whereas the magnetic properties are dominated by the antiferromagnetic Cu-O-Cu interactions along the nearest-neighbor [100] direction. In addition, we predict the second tetragonal CuO phase with a c/a ratio <1 with a different antiferromagnetic ordering and a similar high T_N. We suggest that this phase could be synthesized by epitaxial growth.

DOI: 10.1103/PhysRevB.80.094527 PACS number(s): 74.25.Jb, 71.15.Mb, 74.72.−h, 75.10.−b

I. INTRODUCTION

The interest in the Cu-O alloy system has always been high. One obvious reason is related to the essential roles played by the Cu-O layers in the fascinating high-temperature superconductivity of cuperates.[1,2] The cuprates are known to possess a quasi-two-dimensional structure consisting of layers of CuO_2 planes intercalated by metallic elements. Although the origin of the superconductivity in cuperates is still not fully understood, one of the essential ingredients in the superconducting mechanism is the existence of a large superexchange interaction[1–4] between spins on the Cu sites in the parent compounds. Thus, it would be interesting to explore if similarly large magnetic interactions also exist in other Cu-O alloys. This could lead to candidates for doping experiments and potential parents of superconductors.

Within this context, the very recent work of Siemons *et al.*[5] reporting on the synthesis of tetragonal CuO (elongated rocksalt structure with a c/a ratio of 1.352), which was epitaxially grown on a $SrTiO_3$ substrate, is intriguing, because tetragonal CuO potentially represents the simplest structure with large superexchange interactions. From both technological and fundamental scientific point of view, the synthesis of such a distorted rocksalt-type copper oxide deserves particular attention because a very large Neél temperature T_N can possibly be attained. In fact, extrapolating the linear trend for T_N for transition-metal rocksalt monoxides (MnO: $T_N=118$ K, FeO: $T_N=200$ K, CoO: $T_N=291$ K, and NiO: $T_N=523$ K), the rocksalt CuO would have $T_N \approx 800$ K, as our results indeed confirm. Therefore, a reliable and accurate description of its ground-state electronic and magnetic properties, as we provide in this work, is of great importance. With such a strong antiferromagnetic (AFM) coupling predicted by our calculations, this high-symmetry tetragonal phase of CuO would provide an interesting playground in comparison with superconducting cuprates.[6,7]

Through hybrid density-functional theory,[8] we explore the electronic and magnetic ground-state properties of tetragonally distorted rocksalt CuO. We predict that the tetragonal CuO phase with $c/a=0.846$ (called TET1) and a very large $T_N=1007$ K, which might be grown under suitable experimental conditions. In addition, we predict the existence of a second tetragonal phase of CuO with $c/a=1.377$ (called TET2) is an antiferromagnetic semiconductor with a high $T_N=865$ K and a charge-transfer gap of $E_g=2.7$ eV. This TET2 phase is in good agreement with the recent experiment.[5]

In Sec. II, the computational methodology is briefly described. In Sec. III, we present and discuss our results. A summary is given in the last section.

II. METHOD

Considering that standard density-functional theory (DFT) based approaches describes monoclinic CuO as a diamagnetic metal,[9] their application to the CuO phase considered here would provide a wrong microscopic picture. Therefore, in the present work, we apply hybrid density-functional theory[8] based on the Heyd-Scuseria-Ernzerhof (HSE) method[10] as implemented in the Vienna *ab initio* simulation package (VASP).[11–13] Unlike standard DFT, HSE employs an admixture of Hartree-Fock and Perdew-Burke-Ernzerhof[14] exchange in the construction of the many-body exchange (x) and correlation (c) functional,

$$E_{xc}^{\mathrm{HSE}} = \frac{1}{4}E_x^{\mathrm{HF,sr},\mu} + \frac{3}{4}E_x^{\mathrm{PBE,sr},\mu} + E_x^{\mathrm{PBE,lr},\mu} + E_c^{\mathrm{PBE}}, \quad (1)$$

where (sr) and (lr) refer to the short- and long-range parts of the respective exchange interactions whereas μ controls the range separation of the Coulomb kernel, varying between 0.2 and 0.3 Å^{-1}. We have used $\mu=0.2$ Å^{-1}. The HSE functional is largely self-interaction free thus improving over the standard DFT description and enables us to achieve a correct understanding of strongly correlated electronic systems.[15,16]

In addition to the ferromagnetic (FM) solution, five selected antiferromagnetic orderings are studied: AFM1 with a

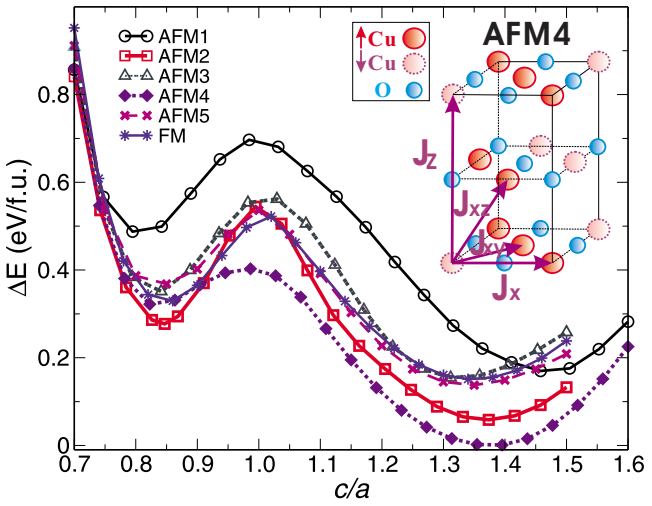

FIG. 1. (Color online) Distortion energy ΔE for a tetragonally distorted rocksalt structure of CuO as a function of c/a at for a variety of magnetic configurations (details, see text); the energy minima for $c/a=0.846$ and $c/a=1.377$ correspond to the TET1 and TET2 structures, respectively. Inset: structure of the TET2 phase with AFM4 ordering; large and small balls denote Cu and O atoms, respectively. Arrows represent the four spin-exchange coupling directions considered in the Heisenberg model (see text).

spin-wave vector of $q=(0.5,0.5,0.0)$, AFM2 with $q=(0.5,0.5,0.5)$, AFM3 with $q=(0.0,0.0,0.5)$, AFM4 ordering as illustrated in Fig. 1, and AFM5 with $q=(0.5,0.0,-0.5)$. The AFM5 ordering corresponds to the experimental magnetic ground state of monoclinic CuO.[17] In order to accurately derive the exchange parameters (cf., Fig. 1), we made use of the same 64-atom supercell with $4\times4\times4$ mesh for all six magnetic orderings for the energy-lowest TET1 and TET2 magnetic phases.

III. RESULT AND DISCUSSION

The structurally optimized total energies as a function of the c/a ratio for the rocksalt structure are shown in Fig. 1 for five different AFM orderings as well as for the FM ordering. We identify two distinct energy minima, namely, for $c/a=0.846$ (TET1) and for $c/a=1.377$ (TET2). The magnetic phase TET1 orders according to AFM2 but TET2 according to AFM4.

The optimized structural parameters are reported in Table I. The value of $c/a=1.377$ for TET2 agrees remarkably well with the experimental value of 1.357. The TET2 phase was epitaxially grown on $SrTiO_3$ with its cubic lattice parameter of $a=3.905$ Å, which provides an ideal lattice-matching condition for tetragonal CuO. Additionally, we speculate that the predicted TET1 CuO phase with its lattice parameter of $a=4.41$ Å, might be grown on a suitable substrate with perovskitelike symmetry and a similar planar lattice constant. Promising candidates are $BaBiO_3$ ($a=4.37$ Å) or the the less-common materials $BaUO_3$ ($a=4.404$ Å) and $BaCeO_3$ ($a=4.44$ Å).

Before discussing the tetragonal TET1 and TET2 phases, it is instructive to recall the basic bonding properties of

TABLE I. Calculated lattice parameters (a,c), local magnetic moment of Cu(m_{Cu}), and band gap (E_g) for the TET1 and TE T2 phases, relatively.

	Theory		Expt.[a]
	TET1	TET2	TET2
$a=b$(Å)	4.41	3.908	3.905
c(Å)	3.73	5.381	5.3
c/a	0.846	1.377	1.357
E_g(eV)	1.5	2.7	
$m_{Cu}(\mu_B)$	0.71	0.69	

[a]Reference 5.

monoclinic CuO. Unlike other members of the transition-metal-oxide series, CuO is unstable against a Jahn-Teller distortion and crystallizes in a monoclinic $C2/c$ structure[18] with spin orientations alternating along $[10\bar{1}]$ with $T_N=220$ K (Refs. 17 and 19) and a reported gap of 1.4–1.7 eV (Refs. 21 and 22). The driving force for the formation of the monoclinic structure is the crystal-field splitting of the ideal rocksalt orbital configuration. In fact, in the ideal rocksalt phase, the Cu d_{e_g} orbitals ($d_{x^2-y^2}$ and d_{z^2}) are degenerate and exhibit the configuration $(\uparrow d_{x^2-y^2})^1(\downarrow d_{x^2-y^2})^{0.5}(\uparrow d_{z^2})^1(\downarrow d_{z^2})^{0.5}$. Such an occupation is energetically unfavorable, cannot mimic the intra-atom Coulomb repulsion in the d^9 octahedral environment and ultimately causes a structural transition.

Our HSE approach correctly favors the monoclinic structure as the CuO ground state and we found it to be ≈100 meV/f.u. more stable than the TET2 phase with a gap of 2.1 eV, in agreement with a precedent pseudo-*SIC* (self-interaction-correction) calculation.[20] The Jahn-Teller distortion splits the $d_{x^2-y^2}$ and d_{z^2} states, and the monoclinic crystal field spin polarizes the d_{z^2} states. The partially filled d_{z^2} states hybridize with both, the oxygen p_z orbitals (creating antiferromagnetic alignment along the c axis) as well as with the oxygen p_x,p_y states (generating in-plane Cu-O ferromagnetic coupling).[20]

As shown in Fig. 1, an alternative route to break the degeneracy of $d_{x^2-y^2}$ and d_{z^2} states is the symmetry lowering by tetragonal distortion of the rocksalt structure, and by that the two metastable tetragonal phases TET1 and TET2 are found but with different AFM orderings. The orbital-dependent density of states (DOS) of AFM2-type TET1 and AFM4-type TET2 shown in Fig. 2 demonstrates the lifting of the degeneracy by splitting the states. For tetragonal CuO the Cu^{2+} ions have the same d^9 electronic configuration with a single unpaired d state but the electronic structure of Cu in both structures is intrinsically different because tetragonality affects $d_{x^2-y^2}$ and d_{z^2} states in a different way from the point of view of orbital ordering within the tetragonal crystal field. For TET1, the DOS of $d_{x^2-y^2}$ states are fully occupied whereas d_{z^2} states are splitted into occupied and unoccupied states with a large splitting of about 10 eV. This gives rise to a local magnetic moment of Cu of 0.71 μ_B and a charge-transfer gap of 1.5 eV. The resultant electronic configuration is $(d_{x^2-y^2})^2(d_{yz},d_{xz})^4(d_{xy})^2(d_{z^2})^1$. For the TET2 structure the opposite effect is observed; the d_{z^2} states are fully occupied

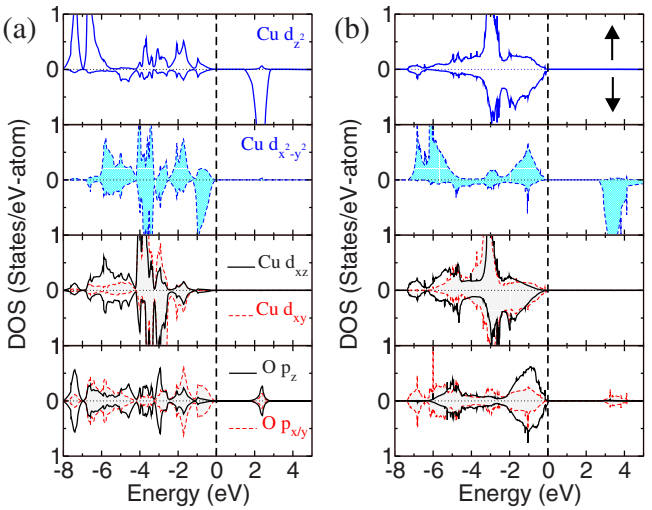

FIG. 2. (Color online) Calculated spin-resolved local density of states of tetragonal CuO. Panel a: TET1 (c/a=0.846) with AFM2 ordering, panel b: TET2 (c/a=1.377) with AFM4 ordering. Because d_{xz} and d_{yz} are degenerated, only the former is shown. The zero energy is set to the top of the valence band.

whereas the spin splitting emerges from the majority and minority $d_{x^2-y^2}$ states resulting in a local magnetic moment of Cu of 0.69 μ_B and a rather large charge-transfer gap of 2.7 eV. Therefore, in the TET2 case the electronic configuration is $(d_{z^2})^2(d_{yz},d_{xz})^4(d_{xy})^2(d_{x^2-y^2})^1$. To illustrate the distinct magnetic polarization of the CuO tetragonal phases, we show the spin-density isosurfaces in Fig. 3. The spin-density plots clearly reflects the d_{z^2} and $d_{x^2-y^2}$ polarization characters for the TET1 and TET2 phases, respectively.

The distinct orbital picture of the TET1 and TET2 phases is intermingled with the different c/a ratio and the concomitant modification of the planar lattice constant in the two tetragonal structures. Upon compression of the c/a ratio (TET1) the planar lattice constant a is stretched considerably up to 4.40 Å (corresponding to a Cu-O bond length of $d_{\text{Cu-O}}$=2.20 Å) whereas the c axis shortened significantly and the bond length along the c axis is reduced to $d_{\text{Cu-O}}$=1.865 Å. The resultant structural anisotropy dominates the chemical bonding: the planar Cu-O hybridization is relatively weak compared with a reinforced Cu d_{z^2} and O p_z

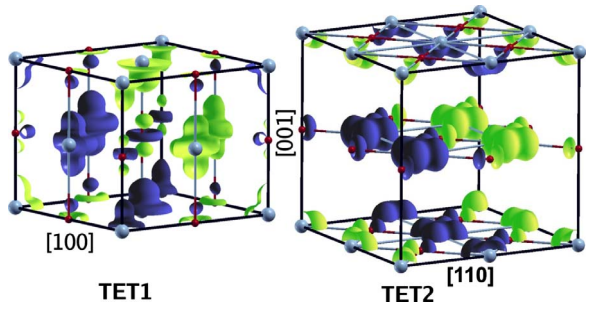

FIG. 3. (Color online) Spin-density isosurfaces for the AFM2 TET1 (c/a=0.846) and AFM4 TET2 (c/a=1.377) phases. Dark and light colored surfaces denote spin-up and spin-down densities whereas large and small spheres are Cu and O atoms, respectively.

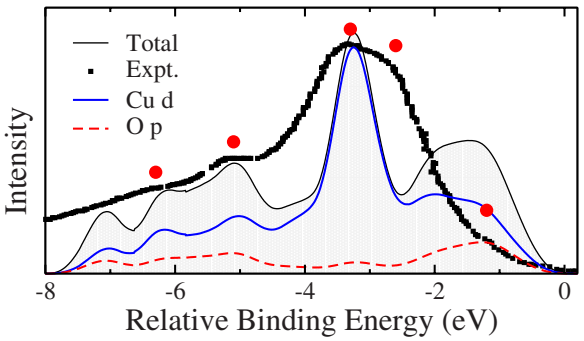

FIG. 4. (Color online) Comparison between HSE calculated density of states and experimental valence-band spectra for the tetragonal AFM4-type TET2 phase of CuO. The filled circles indicate the peak positions, as given by in the experimental work of Ref. 5. The levels of the experimental and calculated valence states have been aligned and the calculated states were convoluted with a Gaussian of width σ=0.2 eV.

hybridization. On the other hand, the TET2 phase experiences an opposite structural anisotropy with a stretched value of c=5.381 Å and a reduced planar lattice constant of a=3.908 Å. As a consequence, $d_{x^2-y^2}$ states strongly hybridize with the oxygen p_x,p_y states, as evident in a large splitting in energy between the bonding and antibonding $d_{x^2-y^2}$ states of Cu (cf. Fig. 2).

The comparison between the calculated DOS of TET2 with the experimental valence-band spectrum shown in Fig. 4 provides further support for our predictions because the experimentally observed peaks (filled circles in Fig. 4) are reproduced well by our simulations. The main peak at −3.5 eV originates from Cu d_{z^2} states which weakly hybridize with O p states whereas the low-energy region below −4 eV consists of $d_{x^2-y^2}$ states strongly hybridized with oxygen p_x,p_y states. The difference between theory and measurement seems to be the DOS peak centered at −1.5 eV, although in the experimental paper[5] a peak is marked at this position. We tentatively attribute the absence (or rather weakness) of this peak to be a surface related effect such as band narrowing due to the reduced coordination of surface atoms. Another difference is that the HSE calculation does not reproduce the experimentally observed peak at −2.5 eV, which is almost as strong as the highest peak at −3.5 eV. Currently, its origin for this difference is unclear. Therefore, more experimental and theoretical investigations are required to clarify this issue.

The magnetic state of tetragonal CuO is a crucial issue because the magnetic interactions determine the range of practical applications and provide fundamental insights in the microscopic understanding. For evaluating the interatomic magnetic exchange interactions, the system is mapped onto an effective Heisenberg spin Hamiltonian $H=-\Sigma_{i\neq j}J_{ij}\mathbf{S_i}\cdot\mathbf{S_j}$. For tetragonal CuO, the spin Hamiltonian can be expressed in terms of the four exchange parameters J_{xy}, J_{xz}, J_x, and J_z as sketched in Fig. 1. The exchange parameters J_{ij} are derived from total-energy calculations for various magnetic orderings (cf. Fig. 1) and listed in Table II. It shows that the structural and electronic anisotropies as discussed above are clearly reflected in the magnetic proper-

TABLE II. Calculated exchange interaction parameters (meV) and Neél temperatures T_N(K) compared to the corresponding theoretical data for monoclinic CuO available in literature. The experimental value of the monoclinic C2/c CuO is T_N(K)=220 K (Ref. 17).

	J_{xy}	J_{xz}	J_x	J_z	T_N
TET1 (c/a=0.846)	−70.0	40.0	−51.6	−197.7	1007
TET2 (c/a=1.377)	63.0	32.3	−159.4	60.5	865
$C2/c$ (Ref. 26)		−3.9	−4.7	−75.0	296
$C2/c$ (Ref. 20)		−14	20.4	−38.4	107

ties. For the TET2 phase, the strongest antiferromagnetic interaction is the Cu-O-Cu superexchange in [100] direction, characterized by a large negative spin interaction J_x=−159.4 meV. The other magnetic interactions are also significant, although their absolute values are predicted to be approximately three times smaller than $|J_x|$. However, for the TET1 phase, the antiferromagnetic Cu-O-Cu superexchange along [001], J_z=−197.7 meV, is by far the dominant one, with its absolute value almost four times larger than the other exchange parameters. Our HSE calculations show that the J_x interaction is the driving force for the AFM4 ordering, for which the antiferromagnetic coupling between nearest Cu atoms via the [100] Cu-O-Cu superexchange is strongly favored, in combination with the ferromagnetic coupling along the c axis. Following similar arguments, one arrives at the conclusion that the superexchange interaction J_z is the driving force for the AFM2 ordering in TET1.

Knowing the exchange parameters J_{ij}, the Neél temperature can be derived within molecular-field theory by $T_N = 2S(S+1)/(3k_B)\Sigma_{i\neq j}J_{ij}$.[23,24] Rescaling T_N's according to Anderson,[25] we obtain the values as listed in Table II which indicate that both tetragonal CuO phases have large values of T_N. Due to the simplifications of molecular-field theory, one cannot expect quantitative agreement with experiments in the estimation of T_N. Nevertheless, in terms of the trend, previous calculations based on the molecular-field theory have been successful in estimating the T_N of monoclinic CuO.[20,26] A direct comparison with the previously reported T_N for monoclinic CuO (Table II) reveals that the tetragonal phases of CuO have much higher Neél temperature than the monoclinic CuO phase. Due to their high-T_N values, the tetragonal phases of CuO might represent interesting candidates for doping treatments, perhaps revealing doping-induced electronic and magnetic modifications with some possible implications for the field of high-T_c superconductivity.[6] Therefore, we are convinced that our finding would serve the good purpose of stimulating more research activities.

IV. SUMMARY

By means of a hybrid density-functional approach we have investigated the bonding properties and magnetic interactions of the recently synthesized tetragonal phase of CuO. In addition to providing microscopic evidence and understanding for the experimental results, such as the bonding character and the size of the tetragonal CuO band gap, we have predicted another tetragonal phase with a c/a ratio =0.846. We suggest that this second tetragonal phase might be grown on suitable substrates such as $BaXO_3$ (X =Bi,U,Ce). For both tetragonal phases we estimate a very large Neél temperature of 800–1000 K, which is considered as one of esstential ingredients in superconducting mechanism. We believe that our predictions will immediately stimulate experimental investigations.

ACKNOWLEDGMENTS

Research at Oak Ridge National Laboratory was sponsored by the Division of Materials Sciences and Engineering, U.S. Department of Energy under contract with UT-Battelle, LLC. This research used resources of the National Energy Research Computing Center, which is supported by the Office of Science of the U.S. Department of Energy. R.P. acknowledges the support of the Austrian *Fonds zur Förderung der wissenschaftlichen Forschung* within the Joint Research Program S90. C.F. was supported in part by the Seventh Framework Programme of the European Community through the ATHENA project.

[1] A. Mourachkine, *Room-temperature Superconductivity* (Cambridge International Science, Cambridge, UK, 2004).
[2] D. M. Newns and C. C. Tsuei, Nat. Phys. **3**, 184 (2007).
[3] O. Chmaissem, J. D. Jorgensen, S. Short, A. Knizhnik, Y. Eckstein, and H. Shaked, Nature (London) **397**, 45 (1999).
[4] H.-B. Yang, J. D. Rameau, P. D. Johnson, T. Valla, A. Tsvelik, and S. D. Gu, Nature (London) **456**, 77 (2008).
[5] W. Siemons, G. Koster, D. H. A. Blank, R. H. Hammond, T. H. Geballe, and M. R. Beasley, Phys. Rev. B **79**, 195122 (2009).
[6] R. J. Birgeneau, C. Stock, J. M. Tranquada, and K. Yamada, J. Phys. Soc. Jpn. **75**, 111003 (2006).
[7] P. M. Grant, J. Phys.: Conf. Ser. **129**, 012042 (2008).
[8] A. D. Becke, J. Chem. Phys. **98**, 1372 (1993).
[9] W. Y. Ching, Y.-Nian Xu, and K. W. Wong, Phys. Rev. B **40**, 7684 (1989).
[10] A. V. Krukau, O. A. Vydrov, A. F. Izmaylov, and G. E. Scuseria, J. Chem. Phys. **125**, 224106 (2006).
[11] G. Kresse and J. Hafner, Phys. Rev. B **48**, 13115 (1993).

[12] G. Kresse and J. Furthmuller, Comput. Mater. Sci. **6**, 15 (1996).
[13] J. Paier, R. Hirschl, M. Marsman, and G. Kresse, J. Chem. Phys. **122**, 234102 (2005).
[14] J. Heyd, G. E. Scuseria, and M. Ernzerhof, J. Chem. Phys. **118**, 8207 (2003).
[15] C. Franchini, V. Bayer, R. Podloucky, J. Paier, and G. Kresse, Phys. Rev. B **72**, 045132 (2005).
[16] C. Franchini, R. Podloucky, J. Paier, M. Marsman, and G. Kresse, Phys. Rev. B **75**, 195128 (2007).
[17] B. X. Yang, T. R. Thurston, J. M. Tranquada, and G. Shirane, Phys. Rev. B **39**, 4343 (1989).
[18] J. B. Forsyth and S. Hull, J. Phys.: Condens. Matter **3**, 5257 (1991).
[19] B. X. Yang, J. M. Tranquada, and G. Shirane, Phys. Rev. B **38**, 174 (1988).
[20] A. Filippetti and V. Fiorentini, Phys. Rev. Lett. **95**, 086405 (2005).
[21] Z.-X. Shen, R. S. List, D. S. Dessau, F. Parmigiani, A. J. Arko, R. Bartlett, B. O. Wells, I. Lindau, and W. E. Spicer, Phys. Rev. B **42**, 8081 (1990).
[22] J. Ghijsen, L. H. Tjeng, J. van Elp, H. Eskes, J. Westerink, G. A. Sawatzky, and M. T. Czyzyk, Phys. Rev. B **38**, 11322 (1988).
[23] J. H. Van Vleck, J. Chem. Phys. **9**, 85 (1941).
[24] N. Lampis, C. Franchini, G. Satta, A. Geddo-Lehmann, and S. Massidda, Phys. Rev. B **69**, 064412 (2004).
[25] P. W. Anderson, Phys. Rev. **115**, 2 (1959).
[26] H.-J. Koo and M.-H. Whangbo, Inorg. Chem. **42**, 1187 (2003).